Role of antiferromagnetic spin axis on magnetic reconstructions at the (111)-oriented $La_{0.7}Sr_{0.3}MnO_3/LaFeO_3$ interface

I. Hallsteinsen,[1,2] A. Grutter,[3] M. Moreau,[1] S. D. Slöetjes,[1,2] K. Kjærnes,[1] E. Arenholz,[2] and T. Tybell[1,*]

[1]*Department of Electronic Systems, NTNU - Norwegian University of Science and Technology, N-7491 Trondheim, Norway*

[2]*Advanced Light Source, Lawrence Berkeley National Laboratory, Berkeley, California 94720, USA*

[3]*NIST Center for Neutron Research, National Institute of Standards and Technology, Gaithersburg, Maryland 20899, USA*

(Received 10 April 2018; revised manuscript received 20 June 2018; published 7 August 2018)

Engineering of emergent properties at oxide interfaces is an exciting route towards realizing oxide electronics. Such properties are often the result of a balance between cooperating and competing mechanisms in the materials which are difficult to decouple. In this paper, we address the interplay between an antiferromagnetic spin axis and the occurrence of magnetic reconstructions at the (111)-oriented $La_{0.7}Sr_{0.3}MnO_3/LaFeO_3$ interface. We report a critical $LaFeO_3$ thickness where we observed a magnetic interface reconstruction with a net switchable Fe moment only for thicknesses less than or equal to 16 d_{111} layers of $LaFeO_3$. A change from an out-of-plane to in-plane antiferromagnetic spin axis is found at the same critical thickness. We ascribe the interfacial moment to a successively decreased out-of-plane canting of the antiferromagnetic spin axis towards the in-plane $La_{0.7}Sr_{0.3}MnO_3$ magnetization at the interface. This points towards the importance of the local antiferromagnetic order interacting with concurrent structural reconstructions to establish a magnetically reconstructed interface.

DOI: 10.1103/PhysRevMaterials.2.084403

I. INTRODUCTION

Emergent electronic and magnetic ground states in ABO_3 perovskite heterostructures result from complex electronic and atomic reconstructions enabled by advancements in thin-film synthesis [1–4]. In such oxides, the nearly degenerate ground state can be altered by small external stimuli, due to the coupling between the spin, orbital, charge, and lattice degrees of freedom [5]. Moreover, discontinuities in chemical potential, crystal symmetry, and exchange interactions at the interfaces give rise to novel behavior confined to the interface [6]. Recently, there has been increased focus on the control of oxygen octahedral rotations and their connectivity across oxide interfaces. The developed oxygen octahedral rotation control has resulted in interface functionalities such as induced ferroelectricity [7], induced ferromagnetism (FM) [8–11], and polar metals [12]. However, the effects of structural reconstructions are often complicated by cooperating mechanisms such as charge transfer [13], orbital reconstructions [11], and exchange interactions. A central question for oxide interface engineering is thus the understanding of how such mechanisms couple and affect the resulting functionality.

In order to investigate the role of the antiferromagnetic (AF) spin axis on emergent interfacial magnetism, we investigate (111)-oriented $La_{0.7}Sr_{0.3}MnO_3$ (LSMO)/$LaFeO_3$ (LFO) heterostructures. Recently, we reported a FM moment of 1.5 μ_B/Fe in LFO at the interface of 16-d_{111}-layer LSMO/16-d_{111}-layer LFO/$SrTiO_3$ (STO) (111). While the bulk of the LFO layer is AF, the observed Fe moment can be reversed with applied magnetic fields such as the Mn moments in the LSMO layer. No charge transfer across the interface is observed, indicating an atomic reconstruction rather than an electronic reconstruction [9]. The magnetic reconstruction is concurrent with an alteration of the oxygen octahedral rotations at the interface, both extending three to five d_{111} layers into the LFO from the interface. In this paper, we show that in LFO/STO (111) the AF spin axis turns from out of plane to in plane at a critical thickness, similar to $La_{0.7}Sr_{0.3}FeO_3$ (LSFO) in (111)-oriented LSMO/LSFO superlattices [14], and we study the orientation of the FM moment in the reconstructed interfacial LFO relative to the AF spin axis in the bulk of the LFO layer using x-ray absorption and neutron reflectometry. We discuss how the AF spin axis canting out of plane for thin samples supports the interfacial magnetic reconstruction.

II. EXPERIMENTAL

STO (111) substrates with a 0.05° miscut were pretreated with buffered hydrogen fluoride and subsequently annealed at 1050 °C in oxygen flow. Epitaxial heterostructures of LSMO/LFO/STO (111) were deposited by pulsed laser deposition at $T = 540$ °C in 35-Pa oxygen pressure. A KrF excimer laser ($\lambda = 248$ nm) with a fluence of ~ 2 J cm^{-2} and repetition rate of 1 Hz was used to ablate LSMO and LFO from stoichiometric targets onto STO at a distance of 45 mm. This procedure results in thermal mode growth with a minimal resputtering of cations [15]. The growth was characterized *in situ* by reflective high-energy electron diffraction (RHEED). One d_{111} layer is defined as the distance between two subsequent layers of B cations in the (111) direction and corresponding to one RHEED oscillation. For a heterostructure of less than 32 d_{111} layers total, clear RHEED oscillations are found throughout the growth of both layers. For thicker heterostructures, the RHEED oscillations vanished during LFO growth, but did not show signs of three-dimensional (3D) growth, and the intensity was recovered during LSMO deposition. The samples were cooled to ambient temperature in 10-kPa oxygen pressure [16,17].

*Corresponding author: thomas.tybell@ntnu.no

The surface morphology was investigated by atomic force microscopy, revealing clear step-and-terrace structures with a root-mean-square roughness on the terraces of 0.07–0.16 nm on 3 μm × 3 μm images. The thickest LFO layers had the largest roughness, though still less than one d_{111} layer, i.e., all films have smooth surfaces. The structural parameters of the heterostructures were characterized using Cu $K\alpha_1$ x-ray diffraction, using a diffractometer equipped with a Göbel mirror, V-groove beam compressor, and 0.2-mm detector slits. The thin films of all thicknesses have an out-of-plane lattice constant consistent with fully strained (111)-oriented films, and no relaxation along the in-plane high-symmetry crystallographic axis is found (see Supplemental Material [18]). X-ray absorption spectroscopy (XAS) was used to characterize the chemical structure of the LFO and LSMO layers. No difference in the Fe and Mn edges was detected as a function of LFO thickness and the spectral line shapes indicated that the Mn and Fe valence does not vary between the different samples. In summary, the growth method leads to a good interface quality for all thicknesses investigated.

Macroscopic magnetic measurements were done by a vibrating sample magnetometer (VSM). For depth-resolved magnetic characterization we employed polarized neutron reflectivity (PNR) using the PBR instrument at the NIST Center for Neutron Research. The samples were cooled from ambient temperature to $T = 50$ K in a 0.7-T magnetic field applied in plane of the film and measured in the same field. The spin of the incident neutrons was polarized parallel or antiparallel to the magnetic field. The non-spin-flip specular reflectivity was measured as a function of wave-vector transfer along the surface normal Q_z. The PNR data were modeled using the REFL1D software package [19,20], fitting both the individual samples independently as well as a collective data set. X-ray magnetic circular dichroism (XMCD) and x-ray magnetic linear dichroism (XMLD) spectroscopy were measured at beamline 4.0.2 at the Advanced Light Source (ALS). The spectra shown were measured in total-electron-yield mode by monitoring the sample drain current. The x rays are incident at 30° to the sample surface for grazing incidence and at 90° to the sample surface for normal incidence. Using a vector electromagnet, XMCD measurements were performed in applied field of ±0.3 T parallel to the x-ray beam. Hysteresis curves are measured by monitoring the Fe and Mn L_3-edge XMCD as a function of applied field. For XMLD measurements, linear polarized x rays with s and p polarization were used, where the difference is defined as $p - s$.

III. RESULTS AND DISCUSSION

Bulk LFO is orthorhombic (space group 62 $Pbnm$ with $a = 5.557$ Å, $b = 5.5652$ Å, and $c = 7.8542$ Å) and a G-type AF with the AF spin axis oriented along the crystallographic a axis [21]. For a thin film deposited on a cubic substrate with (111) surface orientation, the orthorhombic a axis could either lie in plane, aligned with the $\langle 1\bar{1}0\rangle$ directions, or at 55° out of plane, aligned with the $\langle 110\rangle$ directions. To probe the AF order of LFO layers deposited on STO (111) substrates, XMLD was used. All films show XMLD at the Fe edge. Previously, we have reported that ∼90 d_{111}-layer pure LFO/STO(111) films exhibit six in-plane AF axes [22]. Interestingly, a critical thickness is found for the XMLD between 16 and 19 d_{111} layers of LFO, as shown in Fig. 1(a). Heterostructures with LFO thicknesses equal to or less than 16 d_{111} layers of LFO have a positive (negative) dichroism for the $L_{2,3A}$ ($L_{2,3B}$) edge, while for films with more than 16 d_{111} layers of LFO the linear dichroism has the opposite sign. To ensure that this change in XMLD is not due to crystalline effects, all measurements were performed along the same crystallographic axis of the substrate. The change in sign of the dichroism indicates a change of direction of the AF spin axis. Comparisons to reference data [23,24] reveal that for thicknesses equal to or less than 16 d_{111} layers of LFO the AF spin axis has an out-of-plane component, while for films with more than 16 d_{111} layers of LFO the AF spin axis is in plane. This agrees with measurements on (111)-oriented LSFO/LSMO superlattices [14]. Such a transition from an out-of-plane to in-plane AF spin axis is observed for both pure films of LFO/STO (111) and heterostructures of LSMO/LFO/STO (111) [Fig. 1(a)]. DFT calculations indicate that a change of octahedral tilt in the LFO due to the substrate is limited to the first three to four Fe layers. This implies that the AF spin axis transition is not an effect of the interface, but rather an LFO thickness effect. However, we have no indications of a change in the strain or interface roughness state between 16 and 20 d_{111} LFO layers, hence there is no clear structural transition driving the spin reorientation transition.

In order to investigate the emergent Fe moment at the interface, PNR and XMCD were employed. In Fig. 1(b) the magnetic scattering length density (SLD) from PNR is plotted as a function of depth for three LSMO/LFO heterostructures, where the different layers are color coded. The LSMO layer for all films has a positive magnetic SLD, indicating FM order throughout the film. The heterostructures with three and 16 d_{111} layers of LFO have a negative magnetic SLD at the interface, while the heterostructure with 19 d_{111} layers of LFO has no apparent magnetic SLD in LFO. A negative magnetic SLD indicates a macroscopic moment in LFO antiparallel to the magnetization of LSMO. XMCD measurements were performed at the Fe edge as a function of applied magnetic field. In Fig. 1(c) XMCD hysteresis curves at the Fe L_3 edge are shown. A clear switchable moment for Fe for all films with a LFO thickness of 16 d_{111} layers or less is found. For films with a LFO thickness of more than 16 d_{111} layers any XMCD detected is less than 0.5% of the XAS, albeit more pronounced than for pure LFO/$SrTiO_3$(111) samples. We conclude that samples with 16 d_{111} layers of LFO or less have a net Fe magnetic moment at the interface, while thicker LFO samples show little sign of a magnetically reconstructed interface. The XMCD measurements are in agreement with the PNR data, showing a critical thickness between 16 and 19 d_{111} layers of LFO for a magnetic reconstruction of the interface to occur. The critical thickness for the magnetic reconstruction is concurrent with the transition from an out-of-plane to in-plane AF spin axis.

To further investigate the magnetic reconstruction, the magnetization, Curie temperature, coercive field, and anisotropy of the interface state were probed. In Fig. 2(a) the Fe L_3-edge XMCD as a function of LFO thickness is shown. The XMCD signal at the Fe L_3 edge decreases with an increasing thickness of the LFO layer. This indicates a constant magnetic interface layer independent of LFO layer thickness as we are plotting the XMCD relative to the XAS of the whole LFO layer. In Fig. 2(b) the magnetic moment per Fe in saturation obtained by PNR is

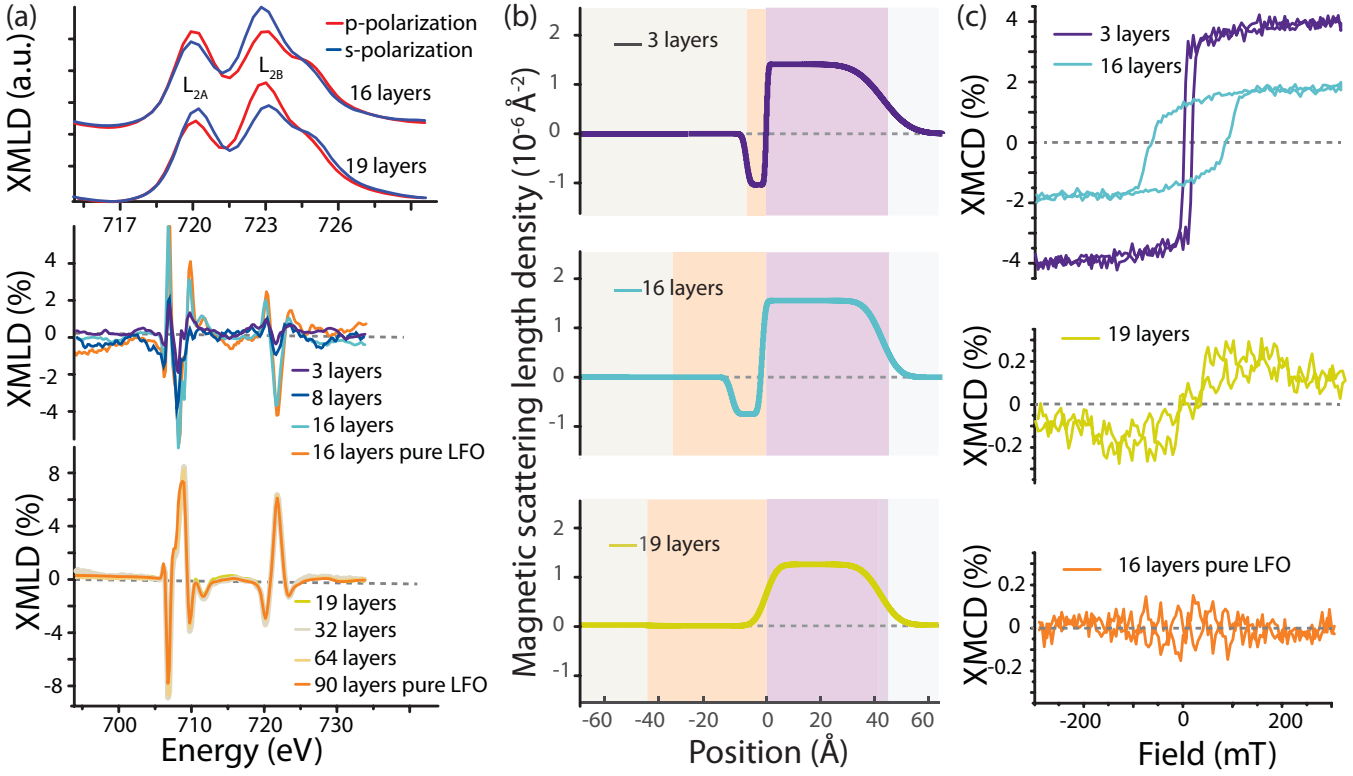

FIG. 1. (a) XMLD L_2 Fe edge for s (blue) and p polarization (red) in grazing incidence for 16 and 19 d_{111} layers of LFO, and XMLD difference relative to XAS for LSMO/LFO heterostructures with different LFO layer thicknesses. Three (purple), eight (blue), and 16 (turquoise) d_{111} layers of LFO have a signature of out-of-plane AF spin axis, while 19 (yellow), 32 (beige), and 64 (light orange) d_{111} layers of LFO have a signature of in-plane AF spin axis. The transition is also found for 16 and 90 d_{111} layers of pure LFO (orange). (b) Depth profile of the magnetic SLD from PNR for three (purple), 16 (turquoise), and 19 (yellow) d_{111} layers of LFO in LSMO/LFO heterostructures. The different layers are color coded, where LSMO is magenta, LFO orange, and STO beige. (c) XMCD hysteresis curves from the Fe L_3 edge for three (purple), 16 (turquoise), and 19 (yellow) d_{111} layers of LFO in LSMO/LFO heterostructures and a pure LFO film of 16 (orange) d_{111} layers. The hysteresis curves are normalized to have positive values for positive fields to more clearly show the hysteric behavior. However, the Fe spin axis is antiparallel to the field in all cases. The measurements for heterostructures with 16 d_{111} layers of LFO are taken from Ref. [9].

shown. For films with a LFO thickness of 19 d_{111} layers or more we get a magnetization of $0.3 \pm 0.4 \mu_B$/Fe, while for films with a LFO layer thickness of 16 d_{111} layers or less the magnetic moment is $1.6 \pm 0.4 \mu_B$/Fe. Unless otherwise noted, all uncertainties and error bars represent a ± 1 standard deviation. This is in agreement with the XMCD measurements showing a magnitude lower and possibly zero interfacial moment above the critical thickness. The constant moment for films with a LFO layer thickness of 16 d_{111} layers or less indicates that the FM moment in LFO is an interface effect. Moreover, PNR shows that the induced magnetization extends three to five d_{111} layers into LFO for all thicknesses. Hence, both PNR and XMCD data suggest that the reconstructed magnetization in LFO is driven by the interface. In Fig. 2(c), the Curie temperatures (T_c) for Mn (LSMO) and Fe (reconstructed LFO) as measured by XMCD and VSM are shown. The T_c measured with XMCD is at a slightly lower temperature than the T_c obtained by VSM. The critical temperature for FM order of the Fe moments coincides with the T_c of the LSMO layer, indicating a magnetic coupling. Interestingly, an increase in Curie temperature for both the LSMO layer and the LFO layer is found for increasing LFO thickness while the LSMO layer thickness does not change.

Comparing the XMCD hysteresis curves for Fe and Mn reveals the moment of Fe is always antiparallel to Mn and the applied field is in agreement with the neutron measurements. In order to check whether the magnetic moment is primarily in plane, XMCD was performed at normal incidence. In Fig. 2(d) a hysteresis curve for the field out of plane for a LSMO/LFO heterostructure with 16 d_{111} layers of LFO is shown. The hysteresis curves change shape with respect to the hysteresis shown in Fig. 1(c), indicative of a magnetically hard axis out of plane. The saturation field is 1 T for the out-of-plane axis, 25 times the size of the in-plane coercive field. Thus, the Fe and Mn moments probed by XMCD hysteresis are primarily aligned in the plane of the film if no external field is applied. In Fig. 2(e) the coercivity for Mn, Fe, and the total film, as measured by XMCD and VSM, is plotted as a function of LFO layer thickness. The coercive fields measured for Fe and Mn are similar to each other for all the heterostructures. The coercivity increases with thickness, followed by a drop in coercivity at the critical thickness, before slightly increasing as the LFO thickness is further increased. We note that for all thicknesses no sign of exchange bias, i.e., a shift of the hysteresis loop along the field axis [25], is observed. The initial increase in coercivity suggests an increasing coupling between the AF and FM layers

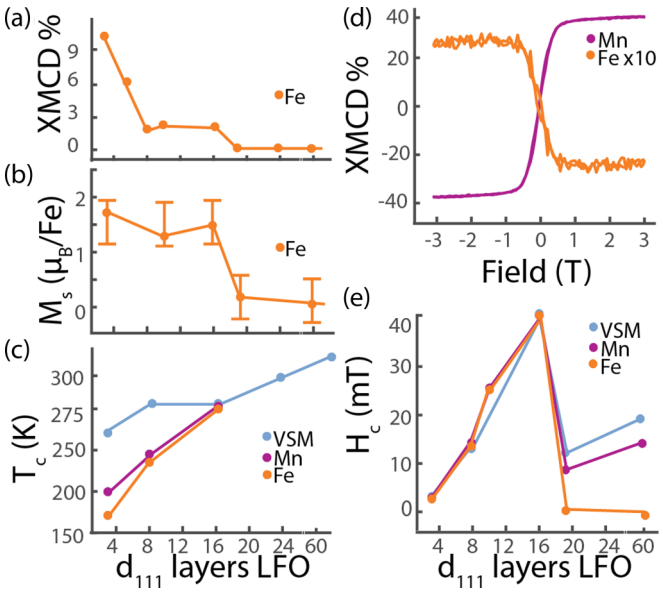

FIG. 2. Magnetic properties of LSMO and the FM moment in LFO as a function of LFO layer thicknesses in LSMO/LFO heterostructures. (a) XMCD relative to XAS in saturation for Fe L_3 edge. (b) Fe magnetic moments in saturation as derived from PNR. The circles represent the best fit of the PNR data, and the error bars the 95% confidence interval. (c) T_c of Mn and Fe L_3 edge measured by XMCD as well as the entire heterostructure as measured by VSM. (d) XMCD hysteresis curves for Mn and Fe L_3 edge of a heterostructure with 16 d_{111} layers of LFO in normal incidence with the magnetic field aligned parallel to the surface normal. (e) Coercive field Mn and Fe from XMCD hysteresis as well as the entire heterostructure as measured by VSM.

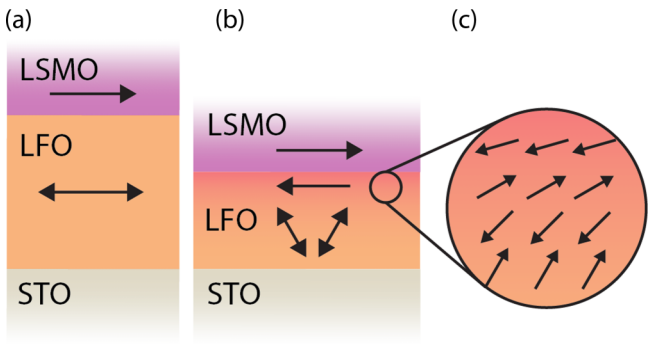

FIG. 3. Schematic of the heterostructure and magnetic spin axis for different LFO layer thicknesses, where STO is colored beige, AF LFO orange, interface reconstructed LFO red, and LSMO magenta, and arrows indicate the spin axis. (a) For heterostructures with more than 16 d_{111} layers of LFO the AFM spin axis lies in plane. (b) For heterostructures with less than or equal to 16 d_{111} layers of LFO the AFM spin axis lies out of plane, while the interface reconstruction has an in-plane FM moment. (c) A possible spin structure of the interface reconstructed area is successively more canted spin-polarized planes, resulting in a net magnetic moment.

as the bulk AF phase grows, while the drop in coercivity at the critical thickness indicates a loss of interfacial coupling at this point. This is in accordance with the interfacial magnetic reconstruction being strongly coupled to both materials.

Figure 3 show a schematic of the spin structures investigated so far. For films with LFO thicknesses of more than 16 d_{111} layers the AF spin axis is in plane and no or little interface magnetization is found [Fig. 3(a)]. For films with LFO thicknesses of 16 d_{111} layers or less the AF spin axis is canted out of plane and an in-plane interface FM moment of $1.6 \pm 0.4 \mu_B$/Fe occurs. As the bulk magnetization of Fe is $4.9 \mu_B$/Fe, the results suggest that the interface LFO layer is not fully FM ordered. A decreased moment indicates that the Fe moments are not parallel aligned, but instead a canted AF or ferrimagnetic order is present. Both scenarios are in agreement with results presented in Ref. [9]. One possibility is shown in Fig. 3(c) where the spin-polarized planes in LFO successively cant toward an in-plane configuration, resulting in a net moment. To investigate the possibility of a canted AF ordering at the interface, we studied the temperature dependence of the XMLD. For all samples the XMLD decreases with increasing temperature as the Néel temperature is approached, and the Néel temperature increases with the number of d_{111} layers of LFO. In Fig. 4(a) the XMLD is plotted as a function of temperature for six (dark blue), eight (light blue), and 16 (turquoise) d_{111} layers of LFO in heterostructures. For all three samples the XMLD signal increases concurrent with the T_c of the interfacial FM moment in LFO. The AF spin axis is out of plane for these thicknesses [Fig. 1(d)], while the FM moments in LFO are in plane [Fig. 2(a)]. A rotation of the interface moments from an in-plane to out-of-plane AF spin axis would lead to an increased XMLD. Hence, when the magnetic interface reconstruction of the Fe moments vanishes, the system becomes fully AF with an out-of-plane spin axis throughout the whole film. To quantify if the in-plane and out-of-plane components of the AF spin axis change with temperature, the difference in intensity for the L_{2A} and L_{2B} edges for s- and p-polarized x rays is analyzed. A 16 d_{111} layers of pure LFO thin film with a mainly out-of-plane spin axis is used as a reference. Figure 4(b) depicts the s- (blue) and p- (red) polarization spectra at 15 K for the reference sample. In grazing incidence, the s-polarized light is parallel to in-plane moments, while the p-polarized light is parallel to out-of-plane moments 60° to the surface. Based on the literature [26], the L_{2B} peak should thus increase for perpendicular spins and decrease for parallel spins. In Fig. 4(b) the spectra for a heterostructure with eight d_{111} layers of LFO at 15 and 200 K is depicted. The increase (decrease) of the L_{2B} peak around the Curie temperature (200 K) for s (p) polarization is indicative of a decreased in-plane component of the AFM spin axis at 200 K as compared to 15 K. Hence, at T_c the AF spin axis cants more out of plane, suggesting the interface moments rotating to the bulk AF ordering.

If the interface reconstructed region (three to five d_{111} layers) has successively canted spin-polarized planes [Fig. 3(c)], the heterostructures with the thinnest LFO thickness should have a larger degree of in-plane AF order as compared to samples with more bulk AF order. In Fig. 4(c) the intensity of the L_{2B} peak (normalized to L_{2A}) is plotted for the two polarizations as a function of LFO layer thickness at 80 K. The 16 d_{111} layers of a pure LFO thin film with a mainly out-of-plane spin axis are used as a reference for s (blue) and p (red) polarization. For p-polarized light (orange circles) the heterostructure with 16 d_{111} layers of LFO is closest to our ref-

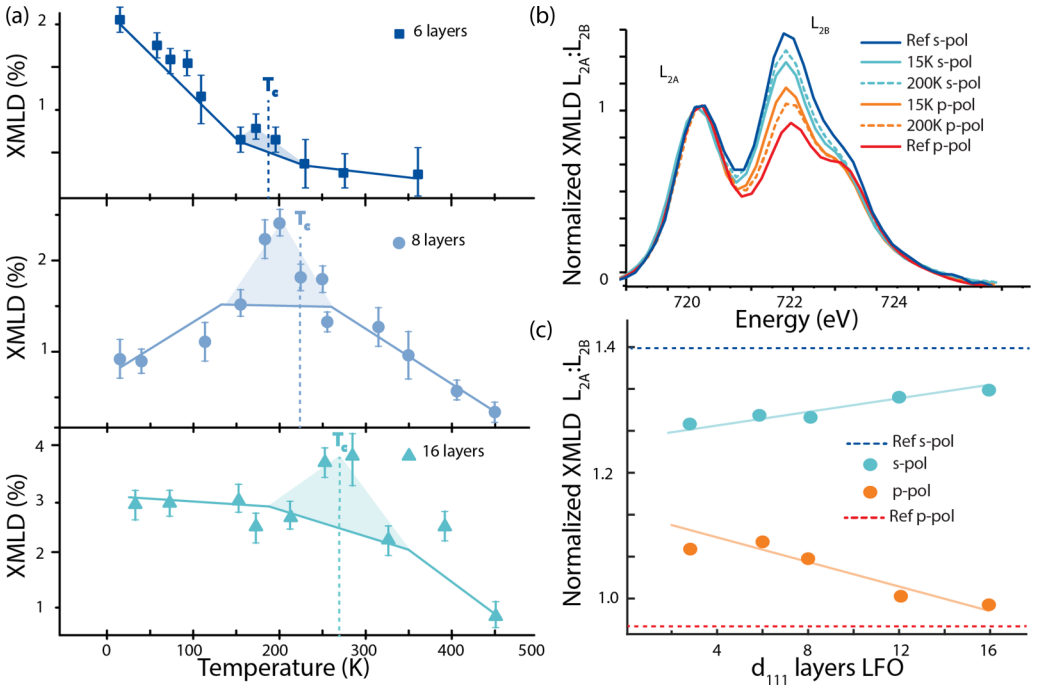

FIG. 4. (a) Magnitude of the XMLD relative to XAS at the Fe L_2 edge as a function of temperature for six (dark blue), eight (light blue), and 16 (turquoise) d_{111} layers of LFO in LSMO/LFO heterostructures. The T_c's of the FM moment of Fe of the samples are indicated with a dotted line. The relative magnitude of the MLD is obtained by fitting the spectra, and the error bars represent the goodness of the fit. The increase in magnitude around the T_c is highlighted with a shaded area for clarity. (b) XMLD spectra normalized to the same intensity of the L_{2A} peak for s- and p-polarized light in grazing incidence. A pure 16-d_{111}-layer LFO thin film at 15 K is used for reference for the out-of-plane spin axis. The plot shows polarization spectra from a LSMO/LFO heterostructure with eight d_{111} layers of LFO at 15 and 200 K. (c) XMLD L_{2B} peak intensity normalized to the L_{2A} peak for heterostructures with LFO layer thicknesses of three to 16 d_{111} layers at 80 K. The red (blue) dotted lines show the magnitude of the reference p (s) polarization from (b) of a pure LFO film with an out-of-plane spin axis. The orange (turquoise) circles indicate the peak intensity for p (s) polarization.

erence sample and hence is mostly out of plane. The L_{2B} peak with p polarization (orange circles) increases with decreasing film thickness. Hence the LSMO/LFO heterostructure with three d_{111} layers of LFO has less out-of-plane AF spin axis of all the thicknesses. For s-polarized light (turquoise circles) the intensity of the L_{2B} peak decreases with decreasing thickness, hence the heterostructures with the smallest LFO thickness have more in-plane character than thicker LFO layers in the heterostructures. By assuming that the reference is totally out of plane, and thickness dependent, the heterostructure with 16 d_{111} layers of LFO has a ∼95% out-of-plane and 5% in-plane AF character, while the heterostructure with three d_{111} layers of LFO has a 75% out-of-plane and 25% in-plane AF character. This change of degree of out-of-plane AF order agrees well with successively canted spin-polarized planes of an interface region of three to five d_{111} layers.

IV. CONCLUSION

In previous work we have established that the structural reconstructions at the LSMO/LFO interface in (111)-oriented heterostructures are concurrent with a net Fe moment in LFO layers near the interface to LSMO [9]. The data presented in the current paper point to the impact of the orientation of the AF spin axis on the magnetic reconstructions. For heterostructures with LFO layer thicknesses equal to or below the critical thickness of 16 d_{111} layers, an induced magnetic moment on the Fe and out-of-plane AF component coexists, while for heterostructures with thicker LFO layers, the induced Fe moment is an order of magnitude smaller and the AF spin axis is in plane. The net Fe moment is always antiparallel to the LSMO magnetization and has an in-plane easy axis. A magnetic reconstructed depth of three to five Fe layers as measured by PNR and a Fe magnetization determined at ∼20% of fully Fe magnetization points towards a canted AF at the interface. The data are consistent with a successively decreased out-of-plane canting of the AF moments towards the interface, which is expected in order to align the Fe moments antiparallel with the in-plane magnetization of LSMO and resulting in the net moment on Fe. The antiparallel alignment of the net Fe moment to the LSMO magnetization is in accordance to earlier reported interface magnetizations between Fe and Mn [10,11].

Our combined PNR and XMCD/XMLD study shows the importance of the AF spin structure for a magnetic interface reconstruction to occur. We have earlier shown that oxygen octahedral rotations are concurrent with the magnetic interface reconstruction. Although the energies associated with magnetic order are smaller than the energy required to induce structural changes such as octahedral rotations, it is clear that in order to fully understand interface magnetic reconstructions, the effects of the local spin axis of an AF material must be included. In the present case, the canting of out-of-plane AF spin-polarized planes is instrumental for the interfacial switchable moment.

ACKNOWLEDGMENTS

The Advanced Light Source is supported by the Director, Office of Science, Office of Basic Energy Sciences, of the U.S. Department of Energy under Contract No. DE-AC02-05CH11231. I.H. acknowledges the Norwegian-American foundation for support. T.T. acknowledges Research Council of Norway Grant No. 231290. Alpha N'Diaye is acknowledged for writing the fitting code for x-ray dichroism data.

[1] J. Chakhalian, J. W. Freeland, A. J. Millis, C. Panagopoulos, and J. M. Rondinelli, Rev. Mod. Phys. **86**, 1189 (2014).
[2] H. Y. Hwang, Y. Iwasa, M. Kawasaki, B. Keimer, N. Nagaosa, and Y. Tokura, Nat. Mater. **11**, 103 (2012).
[3] A. Ohtomo and H. Y. Hwang, Nature (London) **427**, 423 (2004).
[4] M. Gibert, P. Zubko, R. Scherwitzl, J. Íñiguez, and J.-M. Triscone, Nat. Mater. **11**, 195 (2012).
[5] E. Dagotto, Science **309**, 257 (2005).
[6] P. Zubko, S. Gariglio, M. Gabay, P. Ghosez, and J.-M. Triscone, Ann. Rev. Condens. Matter Phys. **2**, 141 (2011).
[7] J. M. Rondinelli and C. J. Fennie, Adv. Mater. **24**, 1961 (2012).
[8] A. J. Grutter, A. Vailionis, J. A. Borchers, B. J. Kirby, C. L. Flint, C. He, E. Arenholz, and Y. Suzuki, Nano Lett. **16**, 5647 (2016).
[9] I. Hallsteinsen, M. Moreau, A. Grutter, M. Nord, P. E. Vullum, D. A. Gilbert, T. Bolstad, J. K. Grepstad, R. Holmestad, S. M. Selbach, A. T. N'Diaye, B. J. Kirby, E. Arenholz, and T. Tybell, Phys. Rev. B **94**, 201115 (2016).
[10] F. Y. Bruno, M. N. Grisolia, C. Visani, S. Valencia, M. Varela, R. Abrudan, J. Tornos, A. Rivera-Calzada, A. A. Ünal, S. J. Pennycook, Z. Sefrioui, C. Leon, J. E. Villegas, J. Santamaria, A. Barthélémy, and M. Bibes, Nat. Commun. **6**, 6306 (2015).
[11] P. Yu, J. S. Lee, S. Okamoto, M. D. Rossell, M. Huijben, C. H. Yang, Q. He, J. X. Zhang, S. Y. Yang, M. J. Lee, Q. M. Ramasse, R. Erni, Y. H. Chu, D. A. Arena, C. C. Kao, L. W. Martin, and R. Ramesh, Phys. Rev. Lett. **105**, 027201 (2010).
[12] T. H. Kim, D. Puggioni, Y. Yuan, L. Xie, H. Zhou, N. Campbell, P. J. Ryan, Y. Choi, J. W. Kim, J. R. Patzner, S. Ryu, J. P. Podkaminer, J. Irwin, Y. Ma, C. J. Fennie, M. S. Rzchowski, X. Q. Pan, V. Gopalan, J. M. Rondinelli, and C. B. Eom, Nature (London) **533**, 68 (2016).
[13] J. Chakhalian, J. W. Freeland, G. Srajer, J. Strempfer, G. Khaliullin, J. C. Cezar, T. Charlton, R. Dalgliesh, C. Bernhard, G. Cristiani, H. U. Habermeier, and B. Keimer, Nat. Phys. **2**, 244 (2006).
[14] Y. Jia, R. V. Chopdekar, E. Arenholz, Z. Liu, M. D. Biegalski, Z. D. Porter, A. Mehta, and Y. Takamura, Phys. Rev. B **93**, 104403 (2016).
[15] I. Hallsteinsen, M. Nord, T. Bolstad, P.-E. Vullum, J. E. Boschker, P. Longo, R. Takahashi, R. Holmestad, M. Lippmaa, and T. Tybell, Cryst. Growth Des. **16**, 2357 (2016).
[16] J. E. Boschker, E. Folven, Å. F. Monsen, E. Wahlström, J. K. Grepstad, and T. Tybell, Cryst. Growth Des. **12**, 562 (2012).
[17] I. Hallsteinsen, J. E. Boschker, M. Nord, S. Lee, M. Rzchowski, P. E. Vullum, J. K. Grepstad, R. Holmestad, C. B. Eom, and T. Tybell, J. Appl. Phys. **113**, 183512 (2013).
[18] See Supplemental Material at http://link.aps.org/supplemental/10.1103/PhysRevMaterials.2.084403 for details.
[19] http://www.ncnr.nist.gov/reflpak.
[20] B. J. Kirby, P. A. Kienzle, B. B. Maranville, N. F. Berk, J. Krycka, F. Heinrich, and C. F. Majkrzak, Curr. Opin. Colloid Interface Sci. **17**, 44 (2012).
[21] T. Peterlin-Neumaier and E. Steichele, J. Magn. Magn. Mater. **59**, 351 (1986).
[22] I. Hallsteinsen, M. Moreau, R. V. Chopdekar, E. Christiansen, M. Nord, P.-E. Vullum, J. K. Grepstad, R. Holmestad, S. M. Selbach, A. Scholl, E. Arenholz, E. Folven, and T. Tybell, APL Mater. **5**, 086107 (2017).
[23] E. Folven, Y. Takamura, and J. K. Grepstad, J. Electron Spectrosc. Relat. Phenom. **185**, 381 (2012).
[24] Y. Jia, R. V. Chopdekar, E. Arenholz, A. T. Young, M. A. Marcus, A. Mehta, and Y. Takamura, Phys. Rev. B **92**, 094407 (2015).
[25] J. Nogués and I. K. Schuller, J. Magn. Magn. Mater. **192**, 203 (1999).
[26] E. Arenholz, G. van der Laan, R. V. Chopdekar, and Y. Suzuki, Phys. Rev. B **74**, 094407 (2006).